Collective and Noncollective Models of NMR Relaxation in Lipid Vesicles and Multilayers †

ARTICLE *in* THE JOURNAL OF PHYSICAL CHEMISTRY B · JUNE 2008

Impact Factor: 3.3 · DOI: 10.1021/jp075641w · Source: PubMed

Collective and Noncollective Models of NMR Relaxation in Lipid Vesicles and Multilayers†

Jeffery B. Klauda‡

Laboratory of Computational Biology, National Heart, Lung and Blood Institute, National Institutes of Health, Bethesda, Maryland 20892

Nadukkudy V. Eldho§ and Klaus Gawrisch

Laboratory of Membrane Biochemistry and Biophysics, National Institute on Alcohol Abuse and Alcoholism, National Institutes of Health, Rockville, Maryland 20852

Bernard R. Brooks and Richard W. Pastor*

Laboratory of Computational Biology, National Heart, Lung and Blood Institute, National Institutes of Health, Bethesda, Maryland 20892

Received: July 18, 2007; In Final Form: October 22, 2007

NMR ^{13}C spin lattice relaxation ($1/T_1$) rates of dipalmitoylphosphatidylcholine (DPPC) bilayers obtained from molecular dynamics simulations of 72 and 288 lipids are compared with each other, with experimental values from large liposomes obtained by magic angle spinning, and with previously published experimental data from small vesicles. The experimental results for multilayers and vesicles at the same frequencies differ only slightly. The simulation results indicate that T_1 relaxation in the 15.1 to 201.2 MHz carbon frequency range and up to 100 Å length scale is dominated by fast isomerizations and slower lipid wobble ($D_\perp \approx 2.5 \times 10^8$ s^{-1}). Rotational diffusion about the lipid long axis (described by $D_{||}$) does not make a substantial contribution to the T_1. Modifications to the acyl chain torsional potential energy function used for the simulations substantially improve agreement with experiment.

1. Introduction

The spin lattice relaxation ($1/T_1$) data of dipalmitoylphosphatidylcholine (DPPC) lipid bilayers obtained by Brown and co-workers[1] have provided a focal point for understanding membrane dynamics for over 25 years. This is because the rates obtained for each carbon j (Figure 1, squares) are well-fit by the very simple form over the frequency range 15.1−125.7 MHz (carbon):

$$(1/NT_1)_j = \tau_j + B_j\omega_C^{-1/2} \quad (1)$$

where τ_j is a fast relaxation time (frequency independent and similar to those observed for liquid alkanes[2]), B_j is a constant (which can be related to the deuterium order parameter), ω_C is the carbon Larmor frequency, and N is the number of protons bonded to the carbon. The fast component of the relaxation rate was associated with gauche−trans isomerization and provided direct evidence that the bilayer interior is similar to liquid alkanes. The intriguing frequency dependence motivated the hypothesis that the "slow" (nanosecond time scale) dynamics arise from collective motions of the bilayer. Motivated by this controversial interpretation, Szabo[3] analyzed the same data with a "model-free" formalism,[4] writing the spectral density for each carbon, $J_j(\omega)$, as

$$J_j(\omega) = (1 - A_j^2)\tau_j + \frac{A_j^2\tau_S}{1 + (\tau_S\omega)^2} \quad (2)$$

where τ_j is the fast relaxation time, A_j^2 is the generalized order parameter for each carbon, and τ_S is a slow relaxation common to all of the aliphatic chain carbons. The high-quality fit (Figure 1, dotted lines) demonstrated that apparent $\omega_C^{-1/2}$ dependence may be obtained from a functional form not obviously related to collective motions, at least in this frequency range. Subsequent analysis based on Brownian dynamics (BD) simulations of a lipid chain in a mean field[5] and fits to the NMR data[6] supported an alternative hypothesis: that the slow relaxation time is associated with single molecule restricted rotational diffusion or "wobbling in a cone".[7] Physically, this could arise if the internal motions are rapid and average to an effective cylindrical shape for the lipid. The cylinder then rotationally diffuses in a potential of mean torque as if it were a rigid body with a unique rotational diffusion tensor. More recent ^2H NMR measurements by Brown and co-workers[8−10] on dimyristoylphosphatidylcholine (DMPC) indicate that eq 2 leads to deviations from the $\omega_C^{-1/2}$ dependence at lower frequencies and thereby challenges the noncollective model. However, the spectral density associated with restricted rotational diffusion is not simply associated with a single decay time. As described further below, an approximate analytic treatment[11] of a cylinder in an orienting potential yields a correlation function with 9

† Part of the "Attila Szabo Festschrift".

* To whom correspondence should be addressed. E-mail pastorr@nhlbi.nih.gov.

‡ Present address: Department of Chemical and Biomolecular Engineering, University of Maryland, College Park, MD 20742.

§ Present address: Department of Biochemistry & Molecular Biology Medical University of South Carolina 173, Ashley Ave, BSB 733 Charleston, SC 29425.

10.1021/jp075641w CCC: $40.75
Published on Web 01/08/2008

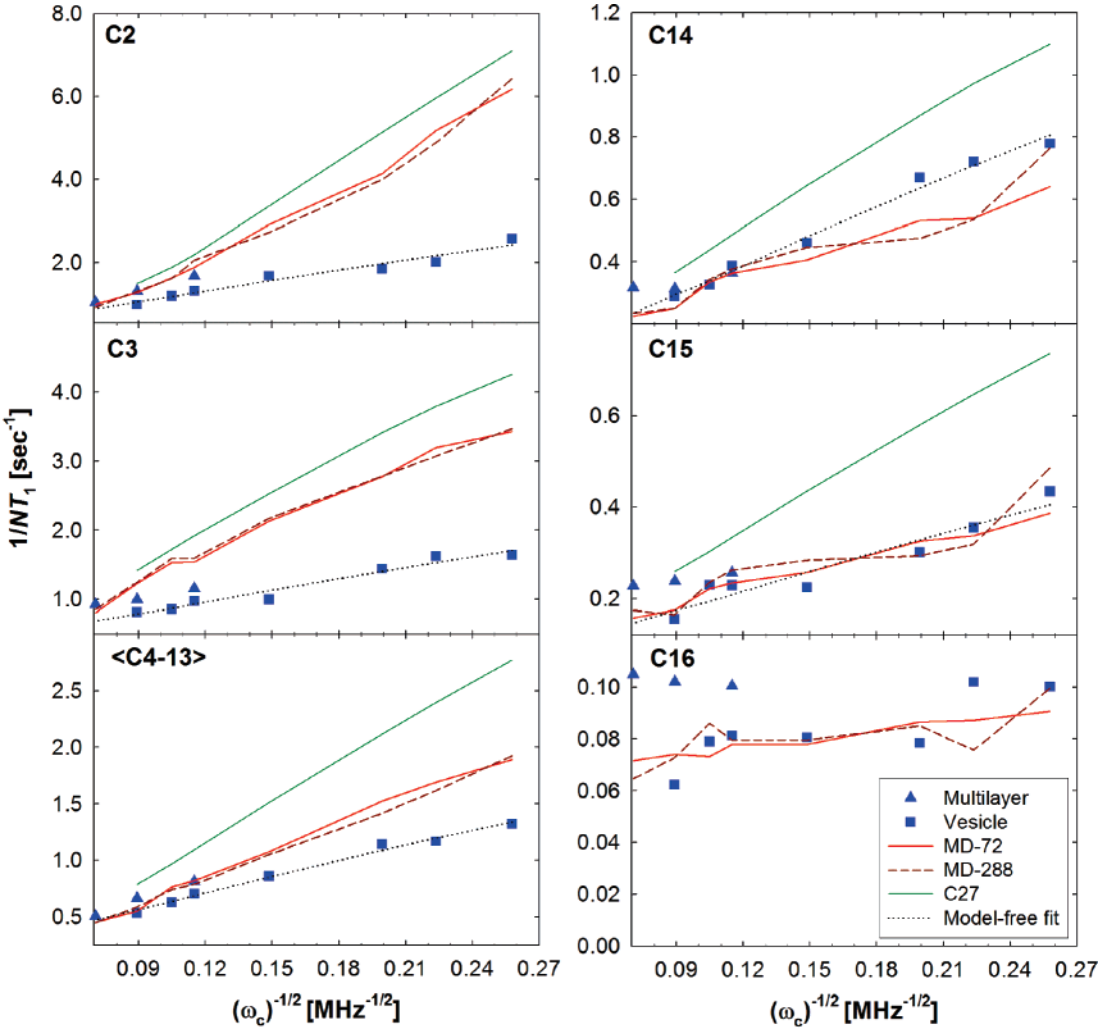

Figure 1. $1/NT_1$ vs $\omega_C^{-1/2}$ for assorted acyl chain carbons of DPPC from experiment (multilayers at ω_C = 75.4, 125.7, and 201.2 MHz, and sonicated vesicles at 15.1−125.7 MHz[1]); MD simulations (solid and dashed lines); and a model-free fit to the vesicle data (dotted lines). Present simulations were carried out with the force field C27r with 72 (MD-72) and 288 lipids (MD-288); C27 denotes results from a previously published simulation[13] carried out with 72 lipids using the C27 force field. Note that the scale for each panel is different.

decay times. Hence, even a poor fit of eq 2 to frequency-dependent data does not, a priori, eliminate the wobble model.

Molecular dynamics (MD) simulations can, in principle, lend insight to the physical origin of the T_1 and the applicability of different models of relaxation. MD simulations of DPPC bilayers have confirmed the alkane-like nature of the fast motions[12] and have shown that the chains do in fact average to a cylindrical shape.[13] However, simulations have been unable to quantitatively reproduce the frequency dependence;[13,14] our previously published results[13] based on the CHARMM C27 force field[15] are included in Figure 1 (green lines). The discrepancy of simulation and experiment can be explained in three ways: (1) the force field (FF) is inadequate; (2) the simulation systems (64 lipids for ref 14 and 72 for ref 13) are too small to support collective motions; or (3) the experimental data on small sonicated vesicles do not correspond to the simulated geometry (a flat system with periodic boundary conditions). This paper presents two classes of results germane to these possibilities: simulated ^{13}C T_1 obtained with a more recently developed FF for systems of 72 and 288 lipids to explore FF and system-size dependencies; T_1 from magic angle spinning (MAS) ^{13}C NMR for large multilayer vesicles at 75.4, 125.7, and 201.2 MHz to probe bilayer geometries arguably closer to those in the simulations and at a higher frequency than previous measurements. In addition, experimental T_1 are reported for the glycerol, choline, and carbonyl carbons at the preceding frequencies.

2. Methods

MD simulations of DPPC at full hydration (30.4 waters/lipid) were carried out at 50 °C at a constant surface area equal to the experimental value of 64 Å^2/lipid.[16] The 72 lipid system was simulated with CHARMM[17] (chemistry at Harvard macromolecular mechanics), and the 288 lipid system was simulated with NAMD[18] using the C27r lipid FF[19] and TIP3P water model.[20,21] The difference between C27r and C27 (used in previous estimates of the T_1 noted above) is the torsional potential on the acyl chains (Figure 2); all other terms are identical. See ref 22 for further details.

T_1 were calculated assuming pure dipolar relaxation between the ^{13}C nucleus and its N attached protons[4]

$$\frac{1}{NT_1} = \frac{1}{10}\left(\frac{\hbar\gamma_c\gamma_h}{r_{C-H}^3}\right)^2 [J(\omega_H - \omega_C) + 3J(\omega_C) + 6J(\omega_H + \omega_C)] \quad (3)$$

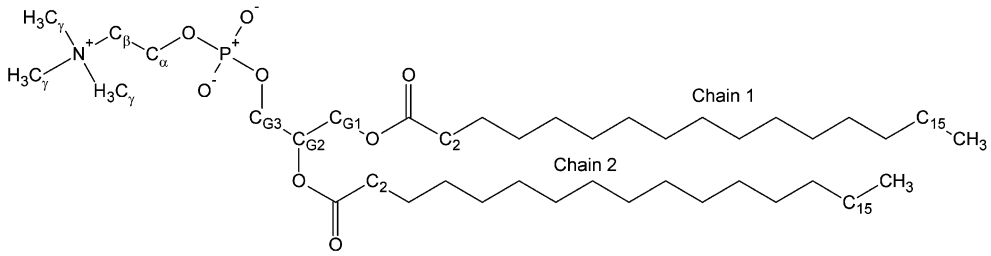

Figure 2. Structure and nomenclature for dipalmitoylphosphatidylcholine (DPPC).

TABLE 1: Experimental and Simulated[a] T_1 (Seconds) for DPPC Multilayers for Three Carbon Frequencies at 50 °C

		75.4 MHz		125.7 MHz		201.2 MHz	
section	carbon	expt	MD	expt	MD	expt	MD
choline	α	0.38	0.32 (0.01)[b]	0.46	0.45 (0.01)	0.54	0.54 (0.03)
	β	0.41	0.31 (0.01)	0.50	0.41 (0.01)	0.58	0.52 (0.03)
	γ	0.64	0.51 (0.02)	0.67	0.53 (0.02)	0.69	0.58 (0.01)
glycerol	G3[c]	0.15	0.14 (0.01)	0.22	0.24 (0.02)	0.31	0.39 (0.04)
	G2	0.18	0.25 (0.02)	0.31	0.48 (0.02)	0.50	0.79 (0.05)
	G1[c]	0.12	0.12 (0.01)	0.18	0.25 (0.01)	0.30	0.36 (0.02)
chains	carbonyl	2.11		1.58		1.16	
	C2	0.30	0.25 (0.01)	0.38	0.39 (0.01)	0.48	0.52 (0.03)
	C3	0.43	0.32 (0.01)	0.50	0.40 (0.01)	0.54	0.60 (0.04)
	C⟨4−13⟩	0.62	0.62 (0.03)	0.75	0.88 (0.04)	0.99	1.11 (0.04)
	C14	1.37	1.37 (0.08)	1.59	2.00 (0.07)	1.58	2.17 (0.14)
	C15	1.95	2.02 (0.10)	2.11	2.93 (0.15)	2.20	3.02 (0.21)
	C16	3.27	4.23 (0.13)	3.32	4.55 (0.13)	3.18	4.90 (0.44)

[a]Simulated values are averaged over trajectories of 72 and 288 lipids. [b] Standard errors for simulations in parentheses. Experimental errors (from fitting and instrumental) are approximately 10% for G1, G2, and G3, and 5% for all other carbons. [c] Assignment of G1 and G3 could be switched because their chemical shifts are nearly identical.

where, $\hbar$ is Plank's constant divided by 2π; r_{C-H} is the effective C−H bond length,[23] 1.117 Å; γ_H, γ_C, ω_H, and ω_C are the gyromagnetic ratios and Larmor frequencies (in radian/s), respectively, of the ^{1}H and ^{13}C nuclei; $\omega_C = \gamma_C H$ and $\omega_H = \gamma_H H$, where H is the field strength. $J(\omega)$ is the spectral density of the second rank reorientational correlation function:

$$J(\omega) = \int_0^\infty \langle P_2(\hat{\mu}(0)\cdot\hat{\mu}(t))\rangle \cos(\omega t)\, dt \qquad (4)$$

where P_2 is the second-order Legendre polynomial and $\hat{\mu}(t)$ is the unit vector along the CH bond direction at time t. Spectral densities were calculated by numerical integration (as opposed to multiexponential fits) of the second rank reorientational correlation functions obtained from four 50 ns trajectories (three of 72 lipids and one of 288 lipids).

The ^{13}C MAS NMR experiments were carried out at 50 ± 2 °C on Bruker AV800, DMX500, and DMX300 spectrometers at resonance frequencies of 201.2, 125.7, and 75.4 MHz, respectively. The sample temperature inside the spinning MAS rotor was calibrated by recording spectra of a series of lipids with known phase transition temperatures. Spin−lattice relaxation times, T_1, were measured at a MAS spinning frequency of 10 kHz by the inversion−recovery pulse sequence (d_1-180°-τ-90°-acquire), a delay time d_1 = 11.5 s, a 5.5 μs 90° pulse, and a spectral width of 27.7 kHz. The experiments were conducted with 50 kHz of proton noise decoupling during data acquisition at 75.4 and 125.7 MHz and with 22 kHz decoupling at 201.2 MHz. The nuclear Overhauser enhancement was retained by application of 2 kHz of proton−noise decoupling starting 3 s before the application of ^{13}C pulses. Spectra were processed using a sine-bell window function before Fourier transformation. The baseline was corrected using a polynomial function of fifth order. Signal intensities were fitted to

$$M(\tau) = M(0)(1 - 2\exp(-\tau/T_1)) \qquad (5)$$

with $M(0)$ and T_1 as fit parameters.

The atom naming for DPPC is shown in Figure 2.

3. Results

Table 1 lists the newly obtained T_1 for multilayers and simulation for DPPC (as for the vesicles, only the average of carbons 4−13 is reported); Figure 3 compares results at 201.2 MHz. The overall profile is very well reproduced by simulation. As expected, the T_1 of the acyl chains increase with increasing carbon number. Values for the choline are comparable to the middle and upper parts of the chain. The lowest T_1 are the glycerol group. This region appears to act as a "pivot point" for the local dynamics of the lipid. The frequency dependence is evident from Table 1 and points to the presence of motions with time scales near the inverse of the Larmor frequency.

From Figure 1, the experimental $1/NT_1$ for each carbon from large multilamellar liposomes are, on average, 13% higher than those from small vesicles at 75.4 MHz, and 28% higher at 125.7 MHz. While these differences are relatively small, they are outside experimental error limits and are unlikely to be caused by minor variations of temperature. Rather, differences between experiments must be considered in detail. For example, in a MAS rotor, lipid water dispersions experience tremendous g-forces, about 500 000 × g near the inner surface of the rotor. Since the densities of water and lipid are not the same, they separate until repulsive hydration forces between lipid bilayers stop the removal of water from the interbilayer space leading to mild dehydration. About 15 water molecules per lipid remain between bilayers on the basis of estimates at the present experimental conditions.[24] It is conceivable that this influences relaxation behavior and confounds a direct comparison with data

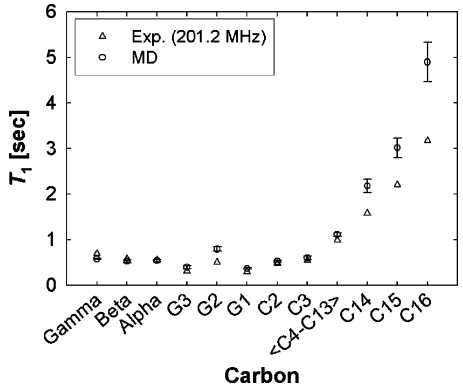

Figure 3. T_1 for all aliphatic carbons of DPPC from simulation and multilayers at 201.2 MHz.

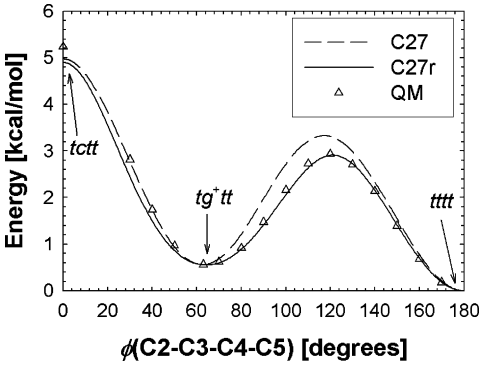

Figure 4. Conformational energies for the C2−C3−C4−C5 dihedral angle of heptane from with all other dihedrals constrained to trans. QM energies are at the CCSD(T)/cc-pVQZ level, and the lines are the surfaces of the empirical potentials C27r and C27 (adapted from ref 19).

from small vesicles. Possible influences from membrane curvature on relaxation should also be considered. Unfortunately, it is difficult to carry out experiments on large multilamellar liposomes at low fields because such magnets are no longer readily available. Consequently, the present experiments cannot be used to infer that relaxations from sonicated vesicles and large multilamellar liposomes are substantially different. Conversely, this implies that the low-frequency vesicle data remain a useful target for simulations.

Turning to the simulations, three trends are evident in Figure 1. First, simulations with C27r with 72 and 288 lipids yield almost identical T_1's in the 15.1 to 201.2 MHz frequency range. While this does not rule out collective motions on longer length or lower frequency scales, it demonstrates that increasing system size from approximately 50 to 100 Å/side does not introduce significant new modes of rotational relaxation. The T_1 for the small and large systems were therefore averaged to yield the more precise estimates shown in Table 1 and Figure 3 and were used for the analysis presented in the next section. This equivalence contrasts our earlier observation for translational diffusion, where system size effects are substantial.[22] In effect, some lipids are displaced when others translate, and a system with only 36 lipids/leaflet is too small. Rotational diffusion of a lipid is less perturbing to its neighbors, and the present system sizes are adequate.

The second trend is that the magnitude and frequency dependence of T_1 from C27r are in substantially better agreement with both multilayer and the vesicle data than those from C27. Given that the only difference between the two FFs is the torsional potential of the acyl chains, the improved agreement with experiment likely arises from a better description of the chain isomerizations and conformational equilbrilia. Figure 4 supports this notion. The trans-to-gauche barrier of C27 is 0.5 kcal/mol higher than indicated by high-level ab initio calculations. This would decrease the isomerization rate compared with experiment, decrease the fast component of T_1, and lead to the overestimate of $1/T_1$. The barrier is reduced for C27r (in accord with the ab initio results), and the agreement with experiment is substantially improved. The change in the frequency dependence is more subtle and is discussed in section 4.

The third trend is that the T_1 from simulations are closer to the multilayer than to the vesicle data. Given that the simulation system is globally flat and thereby closer in shape to large multilamellar liposomes, this result is positive. The very good agreement for carbons in the center of the chain to the terminal methyl group implies that parametrization of the acyl chains is acceptable. The overestimate T_1 at the methyl and neighboring methylene has already been noted for pentadecane[19] and will be considered in future parametrization studies. Agreement of simulation and experiment in the glycerol and choline groups of the lipid is, in general, excellent (Table 1, Figure 3).

TABLE 2: Model-Free Parameters (Eq 2) from a Global Fit of T_1 Obtained from Experimental Vesicle Data,[1] and MD Simulations with the Two Force Fields C27 and C27r

	expt[a], $\tau_S = 1.87$ ns		C27r, $\tau_S = 2.10$ ns		C27, $\tau_S = 2.59$ ns	
carbon	A_j^2	τ_j (ps)	A_j^2	τ_j (ps)	A_j^2	τ_j (ps)
C2	0.0644	46.2	0.2018	35.0	0.2180	53.2
C3	0.0422	35.6	0.0992	55.0	0.1127	69.5
C⟨9−14⟩	0.0382	22.4	0.0586	21.7	0.0788	32.1
C14	0.0248	10.3	0.0167	11.9	0.0296	15.4
C15	0.0107	6.9	0.0091	8.5	0.0190	11.1

[a]Fits to experiment in ref 2 presumed a vibrationally averaged CH distance of 1.1 Å, while those here are based on the more precise value of 1.117 Å. This accounts for the small differences.

4. Discussion

This section discusses the role of the torsional conformational equilibrium in frequency dependence and then focuses on the physical origin of the slow motion.

Frequency dependence in NMR relaxation arises from motions which are on a time scale similar to the inverse of the Larmor frequency. As is easy to see from eq 2, when ω_C is in the 100 MHz range, $\tau_S = 1-2$ ns will yield a substantial frequency dependence. Conversely, when $\tau\omega \ll 1$, $J(\omega)$ and therefore T_1 will be independent of frequency. For example, when $\omega_C = 100$ MHz and $\tau = 100$ ps, $\tau\omega = 0.062$. Hence, it appears counterintuitive that the frequency dependence plotted in Figure 1 for the two parameter sets should differ when the only difference between them is the acyl chain torsional potential (which is associated with "fast" motions). The reason for the change in frequency dependence is that C27r yields an increased fraction of gauche conformations. This can be inferred from Figure 4, where the gauche well is clearly broadened compared to C27. It effectively increases the randomization of orientations by isomerization, decreases the segment order parameter A_j^2, and, from eq 2, decreases the contribution of the slow motion. In the language of model-free analysis, the cone angle restricting the spatial extent of the fast motions is increased.

Table 2 lists the model-free parameters for the simulated T_1. As expected from the change in potential, differences between C27 and C27r are larger in τ_f and A_j^2 than in τ_S. The differences between C27r and the vesicle data are also primarily in the fast motion parameters (the τ_S only differ by 11%). These results

TABLE 3: Parameters from a Fit of Eq 6 to Correlation Functions for Each Carbon from the Four Trajectories Carried Out with C27r

carbon	$D_\perp$ (10^8 s^{-1})	$D_\parallel$ (10^8 s^{-1})	β	S_w^2	S_f^2	τ_f (ps)
C2	1.71	0.00	41	0.597	0.276	41
C3	3.20	0.00	36	0.557	0.256	38
C$\langle$9−14$\rangle$	2.25	0.00	30	0.610	0.133	22
C14	3.03	0.00	28	0.594	0.057	15
C15	2.40	0.00	27	0.624	0.032	14

highlight the role of chain conformation in the observed frequency dependence.

The simulations also provide direct support for the wobble model. Specifically, the second rank correlation functions for each of the CH vectors were fit with the following function

$$C_2(t) = C_w(t) \times C_f(t) \tag{6}$$

$C_w(t)$, the correlation function describing wobble, is given by:[11]

$$C_w(t) = \sum_{m=-2}^{2} g_{m,n}(t) \times \exp[-m^2 t(D_\parallel - D_\perp)](d_{m0}^{(2)}(\beta))^2 \tag{7}$$

where $d_{m0}^{(2)}(\beta)$ are Wigner rotation matrix elements and β is the angle between the vector and the long axis of the cylinder. The $g_{m,n}(t)$ are functions of $D_\perp$ (the rotational diffusion constant of the long axis of the cylinder), $S_w \equiv \langle P_2(\cos\theta)\rangle$ and $\langle P_4(\cos\theta)\rangle$, where P_n are Legendre functions and θ is the instantaneous angle between the cylinder axis and the bilayer normal. $D_\parallel$ is the diffusion constant for rotation about the long axis. The fast decay is modeled with a single-exponential decay constant, τ_f, and order parameter S_f^2:

$$C_f(t) = S_f^2 + (1 - S_f^2)\exp(-t/\tau_f) \tag{8}$$

The underlying assumption of the preceding model is that the rigid body rotation and internal dynamics are uncoupled (eq 6). There is no a priori reason why this should be so. The applicability of the model must be demonstrated by good fits to the simulated correlation functions and consistent parameters.

Table 3 lists the results of fits to the simulated correlation functions. As is necessary for the wobble model, the rigid-body parameters $D_\perp$, $D_\parallel$, and S_w^2 are comparable for each carbon. The slow relaxation is dominated by $D_\perp$, whose average value is 2.5×10^8 s^{-1}. As indicated by eq 7, there is a range of decay times and amplitudes for wobble. The dominant decay varies from 1.0 to 1.9 ns (depending on the carbon), though some decays are on the 100 ps time scale. The fast relaxation parameters S_f^2 and τ_f are different for each carbon and, as expected from the T_1 profile, show increasing flexibility proceeding from the head group to the bilayer center. The relaxation times range from 9 to 55 ps. These are comparable with those obtained in previous MD simulations[12,13] and to the τ_j obtained in the model-free fits for C27r (Table 2). The zero value for $D_\parallel$ indicates that wobble, not axial rotation, dominates the observed decay of the acyl chains.

Geometrical considerations make it difficult to extract $D_\parallel$ from experimental measurements and simulations of the acyl chain carbons. The "ideal" vector for determining $D_\parallel$ is one in which β is close to 90° and S_f^2 is close to 1. Such a vector may not exist for DPPC though could likely be found on other, more rigid, membrane components. These difficulties are likely at the origin of the wide range of values obtained for $D_\parallel$ and $D_\perp$ in other simulation studies;[14,25,26] that is, the values are sensitive to the diffusional model and the vectors used for analysis. When possible, fitting should be carried out on a variety of vectors to test for consistency.

Another source of variation in estimating $D_\parallel$ and $D_\perp$ is the molecular model. For example, our previous analysis[6] of correlation functions from Brownian dynamics of a tethered chain in a mean field[5] yielded the following for DPPC: $D_\perp = 1-2 \times 10^8$ s^{-1}, $D_\parallel = 2 \times 10^{10}$ s^{-1}, and $S_w = 0.5-0.7$. The BD-based $D_\perp$ is in excellent agreement with $D_\perp$ obtained here, suggesting that this is a robust variable. However, the S_w is somewhat lower than reported here, and $D_\parallel$ is far higher. The likely explanation is that internal lipid motions not captured by the tethered chain model are subsumed into an effective $D_\parallel$ and S_w.

5. Conclusions

MD simulations indicate that the ^{13}C T_1 relaxation of the acyl chains of DPPC in bilayers in the 15.1 to 201.2 MHz range and up to 100 Å length scale is dominated by fast isomerizations and slower lipid wobble ($D_\perp \approx 2.5 \times 10^8$ s^{-1}, $\tau_S \approx 2$ ns). Rotational diffusion about the lipid long axis (described by $D_\parallel$) does not make a substantial contribution to the T_1 relaxation. The increased isomerization rates and shifts in conformational equilibrium effected by recent modifications to the CHARMM FF substantially improve agreement with experimental results on multilayers and vesicles. Discrepancies and field dependencies will provide useful targets for future parametrization studies. Simulations of larger systems and for longer times will be required to probe the effects of collective motions.

Acknowledgment. This research was supported in part by the Intramural Research Program of the NIH, National Heart, Lung and Blood Institute. Walter E. Teague assisted conducting the relaxation measurements at 201.2 MHz. We thank Attila Szabo for many helpful discussions over many years.

References and Notes

(1) Brown, M. F.; Ribeiro, A. A.; Williams, G. D. *Proc. Natl. Acad. Sci. U.S.A.* **1983**, *80*, 4325.
(2) Lyerla, J. R., Jr.; McIntyre, H. M.; Torchia, D. A. *Macromolecules* **1974**, *7*, 11.
(3) Szabo, A. *Ann. N.Y. Acad. Sci.* **1986**, *482*, 44.
(4) Lipari, G.; Szabo, A. *J. Am. Chem. Soc.* **1982**, *104*, 4546.
(5) Pastor, R. W.; Venable, R. M.; Karplus, M. *J. Chem. Phys.* **1988**, *89*, 1112.
(6) Pastor, R. W.; Venable, R. M.; Karplus, M.; Szabo, A. *J. Chem. Phys.* **1988**, *89*, 1128.
(7) Kawato, S.; Kinosita, K. *Biophys. J.* **1981**, *36*, 277.
(8) Brown, M. F.; Thurmond, R. L.; Dodd, S. W.; Otten, D.; Beyer, K. *J. Am. Chem. Soc.* **2002**, *124*, 8471.
(9) Nevzorov, A. A.; Trouard, T. P.; Brown, M. F. *Phys. Rev. E* **1998**, *58*, 2259.
(10) Nevzorov, A. A.; Brown, M. F. *J. Chem. Phys.* **1997**, *107*, 10288.
(11) Szabo, A. *J. Chem. Phys.* **1984**, *81*, 150.
(12) Venable, R. M.; Zhang, Y. H.; Hardy, B. J.; Pastor, R. W. *Science* **1993**, *262*, 223.
(13) Pastor, R. W.; Venable, R. M.; Feller, S. E. *Acc. Chem. Res.* **2002**, *35*, 438.
(14) Lindahl, E.; Edholm, O. *J. Chem. Phys.* **2001**, *115*, 4938.
(15) Feller, S. E.; MacKerell, A. D., Jr. *J. Phys. Chem.* B **2000**, *104*, 7510.
(16) Nagle, J. F.; Tristram-Nagle, S. *Biochim. Biophys. Acta* **2000**, *1469*, 159.
(17) Brooks, B. R.; Bruccoleri, R. E.; Olafson, B. D.; States, D. J.; Swaminathan, S.; Karplus, M. *J. Comput. Chem.* **1983**, *4*, 187.
(18) Phillips, J. C.; Braun, R.; Wang, W.; Gumbart, J.; Tajkhorshid, E.; Villa, E.; Chipot, C.; Skeel, R. D.; Kale, L.; Schulten, K. *J. Comput. Chem.* **2005**, *26*, 1781.
(19) Klauda, J. B.; Brooks, B. R.; MacKerell, A. D., Jr.; Venable, R. M.; Pastor, R. W. *J. Phys. Chem. B* **2005**, *109*, 5300.

(20) Jorgensen, W. L.; Chandrasekhar, J.; Madura, J. D.; Impey, R. W.; Klein, M. L. *J. Chem. Phys.* **1983**, *79*, 926.
(21) Durell, S. R.; Brooks, B. R.; Bennaim, A. *J. Phys. Chem.* **1994**, *98*, 2198.
(22) Klauda, J. B.; Brooks, B. R.; Pastor, R. W. *J. Chem. Phys.* **2006**, *125*, 144710.
(23) Ottiger, M.; Bax, A. *J. Am. Chem. Soc.* **1998**, *120*, 12334.
(24) Nagle, J. F.; Liu, Y. F.; Tristram-Nagle, S.; Epand, R. M.; Stark, R. E. *Biophys. J.* **1999**, *77*, 2062.
(25) Essmann, U.; Berkowitz, M. L. *Biophys. J.* **1999**, *76*, 2081.
(26) Moore, P. B.; Lopez, C. F.; Klein, M. L. *Biophys. J.* **2001**, *81*, 2484.